


Dynamical Phase Transitions in Quantum Reservoir Computing

Rodrigo Martínez-Peña[Ⓛ],* Gian Luca Giorgi[Ⓛ], Johannes Nokkala[Ⓛ], Miguel C. Soriano[Ⓛ], and Roberta Zambrini[Ⓛ]†
*Instituto de Física Interdisciplinar y Sistemas Complejos (IFISC, UIB-CSIC),
 Campus Universitat de les Illes Balears, E-07122 Palma de Mallorca, Spain*

 (Received 9 February 2021; revised 11 June 2021; accepted 19 July 2021; published 31 August 2021)

Closed quantum systems exhibit different dynamical regimes, like many-body localization or thermalization, which determine the mechanisms of spread and processing of information. Here we address the impact of these dynamical phases in quantum reservoir computing, an unconventional computing paradigm recently extended into the quantum regime that exploits dynamical systems to solve nonlinear and temporal tasks. We establish that the thermal phase is naturally adapted to the requirements of quantum reservoir computing and report an increased performance at the thermalization transition for the studied tasks. Uncovering the underlying physical mechanisms behind optimal information processing capabilities of spin networks is essential for future experimental implementations and provides a new perspective on dynamical phases.

DOI: [10.1103/PhysRevLett.127.100502](https://doi.org/10.1103/PhysRevLett.127.100502)

Introduction.—Unconventional computing is an interdisciplinary branch of science that aims to uncover new computing and information processing mechanisms in physical, chemical, and biological systems [1]. In this field, the challenge is to develop a device theory guaranteeing that a given system, used as an analog computer, is able to accomplish a computational task. When it comes to solving temporal tasks, a natural “computer” is represented by a system exhibiting rich dynamical properties. An example of such an approach can be found in reservoir computing (RC), an unconventional framework belonging to the broad family of machine learning, derived from recurrent neural networks [2–4] but with the major advantage of low training cost and fast learning. RC is also especially suited for hardware implementations [5–8].

For big-data processing, an exceptional playground where a rich dynamics can be exploited is certainly provided by quantum systems, whose exponentially large number of degrees of freedom pushes them toward computational limits that are not achievable by classical systems [9]. This is the potential envisaged in quantum reservoir computing (QRC) [10,11], as recently explored in spin-based implementations [10,12–15], continuous-variable bosonic systems [16–19], and fermionic setups [20]. Efforts to demonstrate proof-of-principle QRC physical experiments are ongoing [21,22]. Although all the previous works provide examples of functioning quantum reservoir computers, the fundamental issue raised at the beginning remains open: *what conditions must a physical system fulfill to be a good quantum reservoir computer?* The aim of this Letter is to establish the relation between the operation regime of complex computing systems and the performance of QRC.

Networks of interacting spins enable complex dynamics providing a source of memory needed for temporal

tasks in QRC. The time evolution of these systems and the conditions for thermalization have been recently debated in the context of statistical physics. Indeed isolated quantum many-body systems can display thermalization in local observables, as explained by the eigenstate thermalization hypothesis, which can be seen as the manifestation of ergodicity in quantum mechanics [23–25]. A remarkable case of a dynamical regime in which this hypothesis is violated is many-body localization (MBL), where strong disorder causes the emergence of an extensive number of local integrals of motion that break down the thermalization hypothesis [26]. Indeed, such conserved quantities make local observables retain memory of their initial states. Transitions between localization and thermalization manifest in a critical change of a time-averaged order parameter and are referred to as *dynamical phase transitions* [26,27].

The different physical mechanisms underlying the presence or the absence of thermalization deeply influence the computational capabilities of the different dynamical phases. For instance, systems presenting MBL can provide quantum memories at finite temperature [28] and avoid overheating in Floquet systems [29,30]. In quantum machine learning, MBL can improve the trainability of parametrized quantum Ising chains [31]. Contrariwise, localization can be computationally detrimental in quantum annealing [32,33] or quantum random walk algorithms [34,35]. Our work establishes that optimal information processing capabilities in QRC not only are favored in the ergodic phase but also that the onset of this regime can be particularly advantageous. We uncover the underlying physical mechanisms favoring machine learning and also provide a new computing perspective on dynamical phases.

Reservoir layer and dynamical phases.—We choose as a reservoir a spin network described by the transverse-field Ising Hamiltonian plus on site disorder:

$$H = \sum_{i>j=1}^N J_{ij} \sigma_i^x \sigma_j^x + \frac{1}{2} \sum_{i=1}^N (h + D_i) \sigma_i^z, \quad (1)$$

where N is the spin number (from now on we will fix $N = 10$), h is the magnetic field, D_i is the on site disorder, σ_i^a ($a = x, y, z$) are the Pauli matrices, and J_{ij} are the spin-spin couplings, randomly selected from a uniform distribution in the interval $[-J_s/2, J_s/2]$ as is often done in QRC [10,12,13]. D_i will be also randomly drawn from the uniform distribution $[-W, W]$, where W is the disorder strength. For convenience, all the parameters will be expressed in units of J_s .

To characterize the dynamical phases of Eq. (1), we use as usual the ratio of adjacent gaps $r_n = \min[\delta_{n+1}, \delta_n] / \max[\delta_{n+1}, \delta_n]$, where the gaps are $\delta_n \equiv E_n - E_{n-1}$, and $\{E_n\}$ is the sorted list in ascending order of the Hamiltonian eigenvalues [36]. We compute the eigenvalues via exact diagonalization limited to one symmetry sector, as the model possesses a parity (Z_2) symmetry [37]. In the localized phase, the level spacing is expected to display a Poisson distribution with $\langle r \rangle \simeq 0.386$, while in the ergodic phase, according to the random matrix theory, $\langle r \rangle \simeq 0.535$ [48].

The full dynamical phase diagram of Eq. (1) depending on magnetic field strength and disorder is shown in Fig. 1, displaying four different regions: two localization areas (regions I and III, black) and two ergodicity areas (regions II and IV, bright yellow). The localized regime in I corresponds to an MBL paramagnetic phase where the eigenvalue statistics is Poissonian, while region III

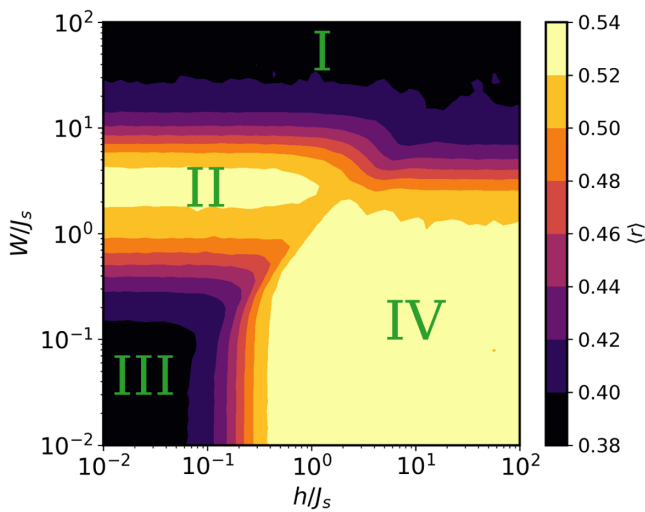


FIG. 1. Heat map of $\langle r \rangle$ for different values of the magnetic field h and the disorder strength W in units of J_s . Results are averaged over 1200 realizations.

corresponds to a spin-glass phase, where the eigenvalue statistics is also Poissonian, but it presents a mobility edge [49]. These regimes have been described in different models as for the transitions III-IV [49–51], IV-I [52,53], or between different localization phases I-II-III [28,54,55]. While such transitions are strictly found in the thermodynamic limit [56,57], signatures are already evident for finite-size systems.

Quantum reservoir dynamics.—The QRC algorithm can be divided into three steps associated with the relative system layers: (i) feed an *input* into the dynamical system; (ii) let the *reservoir*, i.e. the spin network (1), evolve; and (iii) extract information from the reservoir, using all or some of its degrees of freedom via an *output layer* [4]. Let us assume that our input is given by a sequence $\{s_0, s_1, \dots, s_k, \dots\}$ that is injected into the same spin (named qubit 1 for convenience) every time step k [10]. This spin state is updated every Δt as follows: $\rho_1^{(k)} = |\psi_{s_k}\rangle\langle\psi_{s_k}|$, where $|\psi_{s_k}\rangle = \sqrt{1-s_k}|0\rangle + \sqrt{s_k}|1\rangle$, with $s_k \in [0, 1]$. The completely positive, trace-preserving map summarizing the input encoding and information processing is

$$\rho(k\Delta t) = e^{-iH\Delta t} \rho_1^{(k)} \otimes \text{Tr}_1\{\rho[(k-1)\Delta t]\} e^{iH\Delta t}, \quad (2)$$

where $e^{-iH\Delta t}$ is the operator of the unitary dynamics and $\text{Tr}_1\{\cdot\}$ denotes the partial trace performed over the first qubit. The output layer will be built using some of the observables of the system such as the projections $\langle\sigma_i^z\rangle$ of each spin over the z axis or the spin correlations $\langle\sigma_i^z\sigma_j^z\rangle$ (Sec. V in Supplemental Material [37]).

The spin network response to the input injection through the dynamics of the observables $\langle\sigma_i^z\rangle$ provides insightful evidence as shown in Fig. 2. The evolution of the observables in Fig. 2(a) corresponds to the ergodic region (IV in Fig. 1). Colored lines represent the different spins, the input qubit being the blue line. This plot displays that all spin observables are driven to an input-dependent

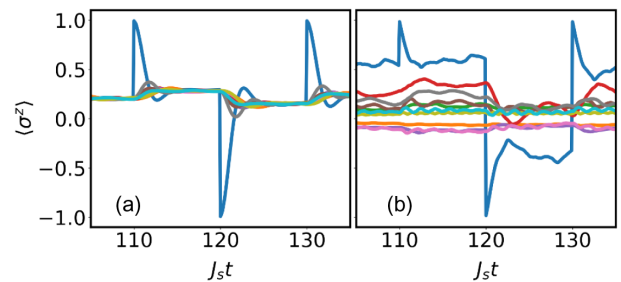


FIG. 2. Dynamics of observables $\langle\sigma_i^z\rangle$ with a binary input ($s_k = \{0, 1\}$). Parameters are (a) $W = 0$, and $h/J_s = 10$; (b) $W/J_s = 10$ and $h/J_s = 1$. We use $J_s\Delta t = 10$ here and in all of the next figures. Input is fed to the first spin (blue line), and the rest of the lines correspond to the other spins. The initial condition is a random density matrix in both (a) and (b).

stationary state within each Δt . The explanation behind this behavior is based on the role of the conserved quantities of the system. In the ergodic regions, total energy $\langle H \rangle$ and parity $\langle P \rangle = \langle \prod_i^N \sigma_i^z \rangle$ are the only conserved quantities, and both of them are delocalized. As detailed in Sec. II of the Supplemental Material [37], their values after the k th input injection [$\langle H(k\Delta t) \rangle$ and $\langle P(k\Delta t) \rangle$] only depend on the initial condition of the system ρ_0 and the input history up to s_k . Then, provided that the unitary dynamics is applied during a time Δt allowing for the eigenstate thermalization, all *local* observables, like $\langle \sigma_i^z \rangle$ in Fig. 2(a), only depend on $\langle H(k\Delta t) \rangle$ and $\langle P(k\Delta t) \rangle$ up to finite-size fluctuations [26]. Therefore, output observables become functions of the input history through $\langle H \rangle$ and $\langle P \rangle$, as for the driven dynamics of Fig. 2(a). We anticipate that resetting the first spin state with the input protocol defined above implies a partial information erasure. Repeating this operation several times amounts to losing all trace of the initial conditions as for the convergence property addressed in the following.

Figure 2(b) corresponds to the transition from ergodic to MBL (regions IV and I, respectively) and displays a significant change of the system response with respect to the previous ergodic case. The observables now show little correlation with respect to the dynamics of the first spin (blue line). This behavior becomes more evident deep in the localized regimes, where none of the $\langle \sigma_i^z \rangle$ are driven by the input, being instead determined by the initial condition [[37], e.g., in the Supplemental Material, Fig. S2(d)]. The physical reason is that the presence of an extensive number of local conserved quantities hinders the information transport across the network. As a prominent effect of MBL, only those conserved quantities involving the first spin are modified by the input, while all the others keep memory of their initial conditions.

Convergence.—A fundamental property a system must exhibit to serve as RC is the convergence or echo state property [2]. This means that, after repeated input injection, the reservoir forgets its initial condition. This is closely related to the so-called fading memory, which is the ability of the output variables to only depend on the recent history of the input sequence [58]. The convergence property is captured by the distance between two different reservoir states after several (here 200) input injections through the protocol in Eq. (2). The initial conditions considered are two random density matrices with a typical distance around $\|\rho_A - \rho_B\| \sim 0.044$ measured using the Frobenius norm, defined as $\|A\| = \sqrt{\text{Tr}(A^\dagger A)}$ [37]. Convergence as a function of h and W is shown in Fig. 3 and exhibits an insightful correspondence with the phase diagram in Fig. 1. Indeed, the convergence property is enhanced in the ergodic phase enabling then the realization of QRC with the spin reservoir in this regime. The influence of different initial conditions persists in the localized phases, which hinders the QRC performance as it will be shown later.

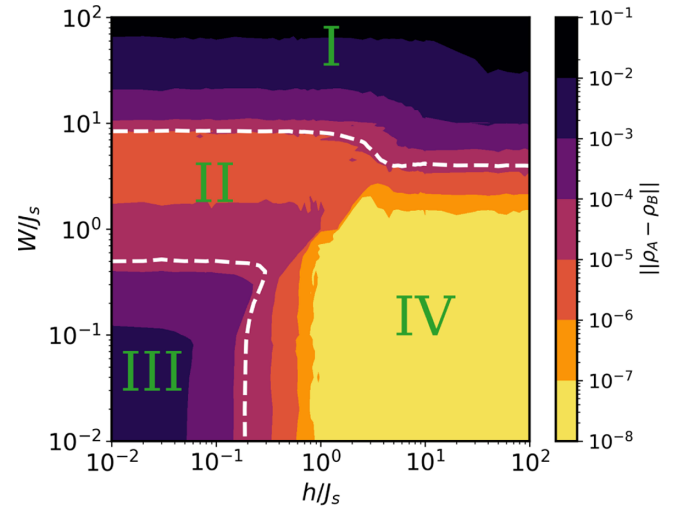


FIG. 3. Convergence of the system for two different (random) initial conditions after 200 inputs. Distance values are averaged over 600 realizations, and those below the threshold of 10^{-8} are kept to this minimum value for clarity. The white-dashed line corresponds to an intermediate value of $\langle r \rangle = 0.46$ in Fig. 1, used to guide the eye.

Even if the map (2) is contractive due to the partial trace, the local conserved quantities make the contractiveness of this dynamical map much weaker than in the ergodic phase. Indeed, in the MBL phase the creation of entanglement between the first qubit and the rest of the network is very weak, as it only grows logarithmically in time [26]. This provides a different focus of dynamical phases, in terms of their response to external perturbations.

RC performance.—While convergence can be seen as a necessary condition to identify suitable RC systems, a characterization of the information processing capabilities of the spin network is needed in order to determine if the reservoir computer can accomplish a given task. A convenient known advantage of RC is that the output layer is the only one that needs to be trained, by optimizing a linear combination of the responses of the reservoir to the task at hand [4]. Given the set of observables \mathbf{x}_k chosen as output, we write the output layer as $y_k = \mathbf{w}^\top \mathbf{x}_k$, where \mathbf{w} are the weights that are adapted by minimizing the error with respect to a target function \bar{y}_k . Training of the output weights \mathbf{w} is usually done using a linear regression [4,37].

To evaluate the reservoir performance, we will consider two different specific tasks as well as a more general indicator for the processing capacity [59]. Let us start with the nonlinear autoregressive moving average (NARMA) model, which is widely used to characterize recurrent neural networks [60]. The general NARMA n task is defined as

$$\bar{y}_k = 0.3\bar{y}_{k-1} + 0.05\bar{y}_{k-1} \left(\sum_{j=1}^n \bar{y}_{k-j} \right) + 1.5s_{k-n}s_{k-1} + 0.1, \quad (3)$$

where n is the maximum delay, \bar{y}_k is the target, and s_k is a random input uniformly distributed, as detailed in Sec. VI of the Supplemental Material [37]. For this task, the quantum reservoir computer needs to learn to emulate Eq. (3) from the random input s_k , i.e., to reproduce a quadratic nonlinear function of the input sequence up to a maximum fixed delay. We fix the maximum delay of Eq. (3) to $n = 10$. In order to address performance both in nonlinear and linear temporal tasks, we also evaluate the linear temporal task $\bar{y}_k = s_{k-\tau}$ fixing $\tau = 10$. The value 10 in both tasks sets the target memory: indeed the reservoir needs a memory of at least ten past inputs at each time step k to solve them. The performance of the spin network for each task can be measured as $C = \text{cov}^2(\bar{\mathbf{y}}, \mathbf{y}) / [\sigma^2(\mathbf{y})\sigma^2(\bar{\mathbf{y}})]$ where cov is the covariance, σ^2 is the variance, and \mathbf{y} and $\bar{\mathbf{y}}$ are the time series of prediction and target, respectively. The performance C is bounded between 0 (target not approximated; the system is useless for this task) and 1 (perfect match between prediction and target).

In this Letter, we benefit from the high dimensionality of the Hilbert phase space of the quantum reservoir by considering an output layer of $O = 75$ observables (going beyond classical RC with one-body observables): all the local spin projections $\langle \sigma_j^x \rangle$, $\langle \sigma_j^y \rangle$ and $\langle \sigma_j^z \rangle$ ($1 \leq j \leq N$), plus the two-spin correlations along the z axis $\langle \sigma_i^z \sigma_j^z \rangle$ ($1 \leq i, j \leq N, i \neq j$). The measurement of these observables is experimentally feasible (Sec. V in Supplemental Material [37]). Figure 4 displays the figure of merit C for the performance of the spin-based reservoir in the NARMA10 and linear memory tasks. In Fig. 4(a), we plot C versus h keeping $W = 0$, while in Fig. 4(b) we fix $h/J_s = 10$ and vary W , in order to detect the change in performance at the transition between different dynamical phases. Localized regimes (regions I and III) show the smallest values of C : the ability to reproduce the target is poor due to their slow convergence properties and actually can be influenced both by the initial elapsed time and the specific choice of initial conditions for the reservoir. In contrast, the ergodic regime (region IV) shows a higher performance achieved rapidly and independently of the reservoir initial state.

Interestingly, in both plots C shows a peak at the transitions between ergodic and localized phases. To show the generality of our results beyond specific tasks and to shed light on the possible performance enhancement at the phase transition, we evaluate [37] the information processing capacity (IPC) [59]. We find that the linear memory builds up first as we move away from the localized phase into the ergodic one. Deep into the ergodic region, nonlinear memory dominates. This trade-off between linear and nonlinear memory brings the performance enhancement at the transition for the NARMA10 task. Although the IPC results indicate that one could find nonlinear tasks where the optimal working point is found in the ergodic region and not at the transition, it is often the case that RC tasks precisely require a combination of linear memory and

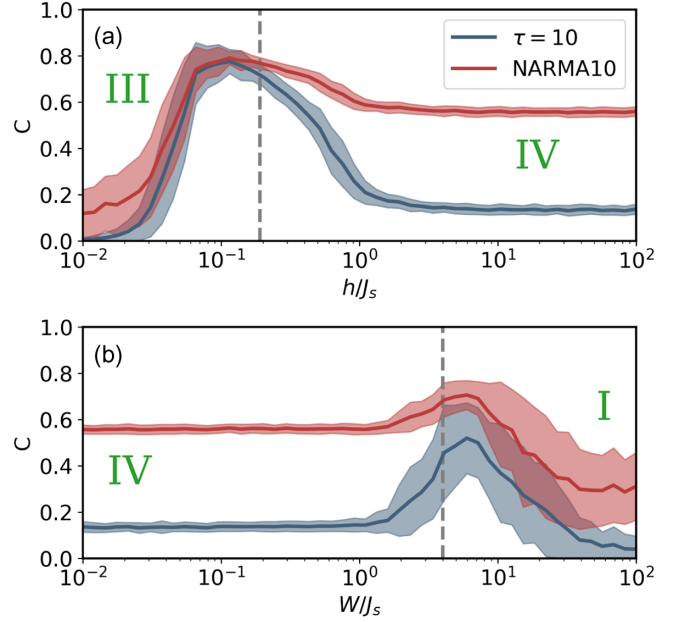


FIG. 4. Performance covariance C for the NARMA10 and linear memory $\tau = 10$ tasks versus h (a) and W (b). We took $W = 0$ for (a) and $h/J_s = 10$ for (b). We represent the average value of C over 100 realizations of the random network with a solid line, while the shadows represent the standard deviation. The gray-dashed line corresponds to the intermediate value $\langle r \rangle = 0.46$ in Fig. 1, used to guide the eye. The initial condition for all the realizations is the maximal coherent state $\rho_0 = (1/2^N) \sum |i\rangle\langle j|$.

nonlinearity, as often reported at the edge of stability between different dynamical regimes [61].

Conclusions.—High performance in QRC can be achieved thanks to the large dimensionality of the Hilbert space. Still, the performance of a system to be used as a quantum reservoir computer crucially depends on its operation regime. We showed in this Letter that localization, because of the presence of local conserved quantities, is detrimental for an optimal information processing performance due to a slow convergence [62]. We demonstrate this in specific tasks as well as in the quantification of the reservoir memory through the IPC. In contrast, the ergodic phase offers a suitable scenario for the convergence property and facilitates efficient information extraction. Different tasks can be solved by exploiting the trade-off between linear and nonlinear memory at the phase transition, and actually the onset of thermalization can be particularly advantageous for QRC, a feature reminiscent of the performance enhancement found in classical RC at the edge of stability [61]. Our QRC study offers an original perspective on thermal and localized phases in terms of their ability to process information and can be further explored in the context of quantum correlations, information scrambling, out-of-time-order correlators [63], and the transient real-time evolution of Loschmidt echoes [27,64].

Furthermore, our results define the proper conditions for experimental implementations of QRC. We showed the importance of tuning the reservoir at the onset of thermalization, which can be easily achieved by controlling the (average) strength of the magnetic field. Another relevant issue concerns the network topology. It is already accepted that random connections are necessary for an optimal performance, avoiding redundancies between different degrees of freedom. But it is not enough. We show that even those topologies with disorder leading to an extensive number of conserved quantities are not suited for RC. Strategies for online data processing addressing quantum measurement [22,65] need to be further explored [37]. The first experiments involve ensemble computing, obtained by taking many copies of the reservoir [21], or rely on the use of nondemolition measurements [22]. Several platforms, ranging from trapped-ion quantum simulators [53,66,67], to optical lattices [68,69] to superconducting circuits [70,71], or photonic simulators [72,73] are mature to establish the potential of QRC toward applications, both for classical and quantum time series processing [11].

We acknowledge the Spanish State Research Agency, through the Severo Ochoa and María de Maeztu Program for Centers and Units of Excellence in R&D (MDM-2017-0711) and through the Quantum Machine Learning Using Reservoir Computing project (PID2019-109094GB-C21 and -C22/AEI/10.13039/501100011033). We also acknowledge funding by Comunitat Autònoma de les Illes Balears through the Machine Learning with Quantum Reservoir Computing project (PRD2018/47). Part of this work has been funded by MICINN/AEI/FEDER and the University of the Balearic Islands through a “Ramon y Cajal” Fellowship (RYC-2015-18140) for M. C. S. and a predoctoral fellowship (MDM-2017-0711-18-1) for R. M. P. Finally, G. L. G. is funded by the Spanish Ministerio de Educación y Formación Profesional/Ministerio de Universidades and cofunded by the University of the Balearic Islands through the Beatriz Galindo program (BG20/00085).

*rmartinez@ifisc.uib-csic.es

†roberta@ifisc.uib-csic.es

- [1] H. Jaeger, Toward a generalized theory comprising digital, neuromorphic, and unconventional computing, *Neuromorphic Comput. Eng.* **1**, 012002 (2021).
- [2] H. Jaeger, The echo state approach to analysing and training recurrent neural networks-with an erratum note, German Natl. Res. Center Inf. Technol. GMD Tech. Rep. **148**, 13 (2001), <https://www.ai.rug.nl/minds/uploads/EchoStatesTechRep.pdf>.
- [3] W. Maass, T. Natschläger, and H. Markram, Real-time computing without stable states: A new framework for neural computation based on perturbations, *Neural Comput.* **14**, 2531 (2002).
- [4] M. Lukoševičius and H. Jaeger, Reservoir computing approaches to recurrent neural network training, *Comput. Sci. Rev.* **3**, 127 (2009).
- [5] L. Appeltant, M. C. Soriano, G. Van der Sande, J. Danckaert, S. Massar, J. Dambre, B. Schrauwen, C. R. Mirasso, and I. Fischer, Information processing using a single dynamical node as complex system, *Nat. Commun.* **2**, 468 (2011).
- [6] G. Van der Sande, D. Brunner, and M. C. Soriano, Advances in photonic reservoir computing, *Nanophotonics* **6**, 561 (2017).
- [7] J. Torrejon, M. Riou, F. A. Araujo, S. Tsunegi, G. Khalsa, D. Querlioz, P. Bortolotti, V. Cros, K. Yakushiji, A. Fukushima *et al.*, Neuromorphic computing with nanoscale spintronic oscillators, *Nature (London)* **547**, 428 (2017).
- [8] G. Tanaka, T. Yamane, J. B. Héroux, R. Nakane, N. Kanazawa, S. Takeda, H. Numata, D. Nakano, and A. Hirose, Recent advances in physical reservoir computing: A review, *Neural Netw.* **115**, 100 (2019).
- [9] F. Arute, K. Arya, R. Babbush *et al.*, Quantum supremacy using a programmable superconducting processor, *Nature (London)* **574**, 505 (2019).
- [10] K. Fujii and K. Nakajima, Harnessing Disordered-Ensemble Quantum Dynamics for Machine Learning, *Phys. Rev. Applied* **8**, 024030 (2017).
- [11] P. Mujal, R. Martínez-Peña, J. Nokkala, J. García-Beni, G. L. Giorgi, M. C. Soriano, and R. Zambrini, Opportunities in quantum reservoir computing and extreme learning machines, *Adv. Quantum Technol.* **4**, 2100027 (2021).
- [12] K. Nakajima, K. Fujii, M. Negoro, K. Mitarai, and M. Kitagawa, Boosting Computational Power through Spatial Multiplexing in Quantum Reservoir Computing, *Phys. Rev. Applied* **11**, 034021 (2019).
- [13] J. Chen and H. I. Nurdin, Learning nonlinear input-output maps with dissipative quantum systems, *Quantum Inf. Process.* **18**, 198 (2019).
- [14] Q. H. Tran and K. Nakajima, Higher-order quantum reservoir computing, [arXiv:2006.08999](https://arxiv.org/abs/2006.08999).
- [15] R. Martínez-Peña, J. Nokkala, G. L. Giorgi, R. Zambrini, and M. C. Soriano, Information processing capacity of spin-based quantum reservoir computing systems, *Cognit. Comput.* (2020).
- [16] S. Ghosh, A. Opala, M. Matuszewski, T. Paterek, and T. C. Liew, Quantum reservoir processing, *npj Quantum Inf.* **5**, 35 (2019).
- [17] S. Ghosh, T. Paterek, and T. C. H. Liew, Quantum Neuro-morphic Platform for Quantum State Preparation, *Phys. Rev. Lett.* **123**, 260404 (2019).
- [18] J. Nokkala, R. Martínez-Peña, G. L. Giorgi, V. Parigi, M. C. Soriano, and R. Zambrini, Gaussian states of continuous-variable quantum systems provide universal and versatile reservoir computing, *Commun. Phys.* **4**, 53 (2021).
- [19] L. C. G. Góvia, G. J. Ribeill, G. E. Rowlands, H. K. Krovi, and T. A. Ohki, Quantum reservoir computing with a single nonlinear oscillator, *Phys. Rev. Research* **3**, 013077 (2021).
- [20] S. Ghosh, T. Krisnanda, T. Paterek, and T. C. H. Liew, Realising and compressing quantum circuits with quantum reservoir computing, *Commun. Phys.* **4**, 105 (2021).
- [21] M. Negoro, K. Mitarai, K. Fujii, K. Nakajima, and M. Kitagawa, Machine learning with controllable quantum

- dynamics of a nuclear spin ensemble in a solid, [arXiv:1806.10910](https://arxiv.org/abs/1806.10910).
- [22] J. Chen, H. I. Nurdin, and N. Yamamoto, Temporal Information Processing on Noisy Quantum Computers, *Phys. Rev. Applied* **14**, 024065 (2020).
- [23] J. M. Deutsch, Quantum statistical mechanics in a closed system, *Phys. Rev. A* **43**, 2046 (1991).
- [24] M. Srednicki, The approach to thermal equilibrium in quantized chaotic systems, *J. Phys. A* **32**, 1163 (1999).
- [25] L. D'Alessio, Y. Kafri, A. Polkovnikov, and M. Rigol, From quantum chaos and eigenstate thermalization to statistical mechanics and thermodynamics, *Adv. Phys.* **65**, 239 (2016).
- [26] D. A. Abanin, E. Altman, I. Bloch, and M. Serbyn, Colloquium: Many-body localization, thermalization, and entanglement, *Rev. Mod. Phys.* **91**, 021001 (2019).
- [27] B. Žunkovič, M. Heyl, M. Knap, and A. Silva, Dynamical Quantum Phase Transitions in Spin Chains with Long-Range Interactions: Merging different Concepts of Non-equilibrium Criticality, *Phys. Rev. Lett.* **120**, 130601 (2018).
- [28] D. A. Huse, R. Nandkishore, V. Oganesyan, A. Pal, and S. L. Sondhi, Localization-protected quantum order, *Phys. Rev. B* **88**, 014206 (2013).
- [29] P. Ponte, A. Chandran, Z. Papić, and D. A. Abanin, Periodically driven ergodic and many-body localized quantum systems, *Ann. Phys. (N.Y.)* **353**, 196 (2015).
- [30] A. Lazarides, A. Das, and R. Moessner, Fate of Many-Body Localization under Periodic Driving, *Phys. Rev. Lett.* **115**, 030402 (2015).
- [31] J. Tangpanitanon, S. Thanasilp, N. Dangniam, M.-A. Lemonde, and D. G. Angelakis, Expressibility and trainability of parametrized analog quantum systems for machine learning applications, *Phys. Rev. Research* **2**, 043364 (2020).
- [32] B. Altshuler, H. Krovi, and J. Roland, Anderson localization makes adiabatic quantum optimization fail, *Proc. Natl. Acad. Sci. U.S.A.* **107**, 12446 (2010).
- [33] C. R. Laumann, R. Moessner, A. Scardicchio, and S. L. Sondhi, Quantum annealing: The fastest route to quantum computation? *Eur. Phys. J. Spec. Top.* **224**, 75 (2015).
- [34] J. P. Keating, N. Linden, J. C. F. Matthews, and A. Winter, Localization and its consequences for quantum walk algorithms and quantum communication, *Phys. Rev. A* **76**, 012315 (2007).
- [35] A. Schreiber, K. N. Cassemiro, V. Potoček, A. Gábris, I. Jex, and C. Silberhorn, Decoherence and Disorder in Quantum Walks: From Ballistic Spread to Localization, *Phys. Rev. Lett.* **106**, 180403 (2011).
- [36] V. Oganesyan and D. A. Huse, Localization of interacting fermions at high temperature, *Phys. Rev. B* **75**, 155111 (2007).
- [37] See Supplemental Material at <http://link.aps.org/supplemental/10.1103/PhysRevLett.127.100502> for additional notes on the dynamics, the convergence properties of the spin network, a note on the experimental implementations, the NARMA task, and the IPC of the system, which includes Refs. [38–47].
- [38] P. Weinberg and M. Bukov, QuSpin: A PYTHON package for dynamics and exact diagonalisation of quantum many body systems part I: Spin chains, *SciPost Phys.* **2**, 003 (2017).
- [39] J. R. Johansson, P. D. Nation, and F. Nori, QuTip: An open-source PYTHON framework for the dynamics of open quantum systems, *Comput. Phys. Commun.* **183**, 1760 (2012).
- [40] E. Ilievski, J. De Nardis, B. Wouters, J.-S. Caux, F. H. L. Essler, and T. Prosen, Complete Generalized Gibbs Ensembles in an Interacting Theory, *Phys. Rev. Lett.* **115**, 157201 (2015).
- [41] R. Vosk and E. Altman, Dynamical Quantum Phase Transitions in Random Spin Chains, *Phys. Rev. Lett.* **112**, 217204 (2014).
- [42] S. D. Geraedts, R. N. Bhatt, and R. Nandkishore, Emergent local integrals of motion without a complete set of localized eigenstates, *Phys. Rev. B* **95**, 064204 (2017).
- [43] V. E. Zbov and A. A. Lundin, On the effect of an inhomogeneous magnetic field and many-body localization on the increase in the second moment of multiple-quantum nmr with time, *JETP Lett.* **105**, 514 (2017).
- [44] K. X. Wei, C. Ramanathan, and P. Cappellaro, Exploring Localization in Nuclear Spin Chains, *Phys. Rev. Lett.* **120**, 070501 (2018).
- [45] P. Richerme, Z.-X. Gong, A. Lee, C. Senko, J. Smith, M. Foss-Feig, S. Michalakis, A. V. Gorshkov, and C. Monroe, Non-local propagation of correlations in quantum systems with long-range interactions, *Nature (London)* **511**, 198 (2014).
- [46] H.-Y. Huang, R. Kueng, and J. Preskill, Predicting many properties of a quantum system from very few measurements, *Nat. Phys.* **16**, 1050 (2020).
- [47] T. Kubota, K. Nakajima, and H. Takahashi, Dynamical anatomy of narma10 benchmark task, [arXiv:1906.04608](https://arxiv.org/abs/1906.04608).
- [48] Y. Y. Atas, E. Bogomolny, O. Giraud, and G. Roux, Distribution of the Ratio of Consecutive Level Spacings in Random Matrix Ensembles, *Phys. Rev. Lett.* **110**, 084101 (2013).
- [49] C. L. Baldwin, C. R. Laumann, A. Pal, and A. Scardicchio, Clustering of Nonergodic Eigenstates in Quantum Spin Glasses, *Phys. Rev. Lett.* **118**, 127201 (2017).
- [50] S. Mukherjee, S. Nag, and A. Garg, Many-body localization-delocalization transition in the quantum Sherrington-Kirkpatrick model, *Phys. Rev. B* **97**, 144202 (2018).
- [51] L. Rademaker and D. A. Abanin, Slow Nonthermalizing Dynamics in a Quantum Spin Glass, *Phys. Rev. Lett.* **125**, 260405 (2020).
- [52] A. O. Maksymov and A. L. Burin, Many-body localization in spin chains with long-range transverse interactions: Scaling of critical disorder with system size, *Phys. Rev. B* **101**, 024201 (2020).
- [53] J. Smith, A. Lee, P. Richerme, B. Neyenhuis, P. W. Hess, P. Hauke, M. Heyl, D. A. Huse, and C. Monroe, Many-body localization in a quantum simulator with programmable random disorder, *Nat. Phys.* **12**, 907 (2016).
- [54] S. Moudgalya, D. A. Huse, and V. Khemani, Perturbative instability towards delocalization at phase transitions between MBL phases, [arXiv:2008.09113](https://arxiv.org/abs/2008.09113).
- [55] R. Sahay, F. Machado, B. Ye, C. R. Laumann, and N. Y. Yao, Emergent Ergodicity at the Transition between Many-Body Localized Phases, *Phys. Rev. Lett.* **126**, 100604 (2021).

- [56] V. Khemani, S. P. Lim, D. N. Sheng, and D. A. Huse, Critical Properties of the Many-Body Localization Transition, *Phys. Rev. X* **7**, 021013 (2017).
- [57] R. K. Panda, A. Scardicchio, M. Schulz, S. R. Taylor, and M. Žnidarič, Can we study the many-body localisation transition? *Europhys. Lett.* **128**, 67003 (2020).
- [58] L. Grigoryeva and J.-P. Ortega, Echo state networks are universal, *Neural Netw.* **108**, 495 (2018).
- [59] J. Dambre, D. Verstraeten, B. Schrauwen, and S. Massar, Information processing capacity of dynamical systems, *Sci. Rep.* **2**, 514 (2012).
- [60] A. F. Atiya and A. G. Parlos, New results on recurrent network training: Unifying the algorithms and accelerating convergence, *IEEE Trans. Neural Networks* **11**, 697 (2000).
- [61] T. L. Carroll, Do reservoir computers work best at the edge of chaos? *Chaos* **30**, 121109 (2020).
- [62] The localized regime shows an extremely much slower convergence than in the ergodic phase. For practical purposes, this is definitely an obstacle for implementing QRC even if strictly speaking convergence would asymptotically be achieved since the map presented in Eq. (2) of the manuscript is contractive due to the partial trace.
- [63] B. Swingle, Unscrambling the physics of out-of-time-order correlators, *Nat. Phys.* **14**, 988 (2018).
- [64] M. Heyl, A. Polkovnikov, and S. Kehrein, Dynamical Quantum Phase Transitions in the Transverse-Field Ising Model, *Phys. Rev. Lett.* **110**, 135704 (2013).
- [65] A. Eddins, J. M. Kreikebaum, D. M. Toyli, E. M. Levenson-Falk, A. Dove, W. P. Livingston, B. A. Levitan, L. C. G. Govia, A. A. Clerk, and I. Siddiqi, High-Efficiency Measurement of an Artificial Atom Embedded in a Parametric Amplifier, *Phys. Rev. X* **9**, 011004 (2019).
- [66] J. Zhang, G. Pagano, P. W. Hess, A. Kyprianidis, P. Becker, H. Kaplan, A. V. Gorshkov, Z.-X. Gong, and C. Monroe, Observation of a many-body dynamical phase transition with a 53-qubit quantum simulator, *Nature (London)* **551**, 601 (2017).
- [67] H. B. Kaplan, L. Guo, W. L. Tan, A. De, F. Marquardt, G. Pagano, and C. Monroe, Many-Body Dephasing in a Trapped-Ion Quantum Simulator, *Phys. Rev. Lett.* **125**, 120605 (2020).
- [68] J.-y. Choi, S. Hild, J. Zeiher, P. Schauß, A. Rubio-Abadal, T. Yefsah, V. Khemani, D. A. Huse, I. Bloch, and C. Gross, Exploring the many-body localization transition in two dimensions, *Science* **352**, 1547 (2016).
- [69] A. M. Kaufman, M. E. Tai, A. Lukin, M. Rispoli, R. Schittko, P. M. Preiss, and M. Greiner, Quantum thermalization through entanglement in an isolated many-body system, *Science* **353**, 794 (2016).
- [70] A. A. Houck, H. E. Türeci, and J. Koch, On-chip quantum simulation with superconducting circuits, *Nat. Phys.* **8**, 292 (2012).
- [71] K. Xu, J.-J. Chen, Y. Zeng, Y.-R. Zhang, C. Song, W. Liu, Q. Guo, P. Zhang, D. Xu, H. Deng, K. Huang, H. Wang, X. Zhu, D. Zheng, and H. Fan, Emulating Many-Body Localization with a Superconducting Quantum Processor, *Phys. Rev. Lett.* **120**, 050507 (2018).
- [72] D. Pierangeli, G. Marcucci, and C. Conti, Large-Scale Photonic Ising Machine by Spatial Light Modulation, *Phys. Rev. Lett.* **122**, 213902 (2019).
- [73] D. Pierangeli, M. Rafayelyan, C. Conti, and S. Gigan, Scalable Spin-Glass Optical Simulator, *Phys. Rev. Applied* **15**, 034087 (2021).